Influence of Doping Concentration and Ambient Temperature on the Cross-Plane Seebeck Coefficient of InGaAs/InAlAs superlattices

Yan Zhang, Daryoosh Vashaee, Rajeev Singh and Ali Shakouri
Electrical Engineering Department, UC Santa Cruz,
1156 High Street, Santa Cruz, CA 95064, USA
Gehong Zeng and Yi-Jen Chiu
Electrical and Computer Engineering Department, UC Santa Barbara, CA 93106, USA

Abstract

We have developed thin film heaters/sensors that can be integrated on top of superlattice microcoolers to measure the Seebeck coefficient perpendicular to the layer. In this paper, we discuss the Seebeck coefficients of InGaAs/InAlAs superlattices grown with Molecular Beam Epitaxy (MBE) that have different doping concentrations, varying between 2e18, 4e18, and 8e18 to 3e19 cm^{-3}. It was interesting to find out that -- contrary to the behavior in bulk material -- the Seebeck coefficient did not decrease monotonically with doping concentration. A preliminary theory of thermoelectric transport in superlattices in the regime of miniband formation has been developed to fit the experimental results. The miniband formation could enhance the thermoelectric power factor (Seebeck coefficient square times electrical conductivity) and thereby improve the Figure of merit, ZT. With this improvement, InGaAs/InAlAs superlattice microcooler become a promising candidate for on-chip temperature control.

Introduction

Lasers and Optoelectronic devices are very sensitive to chip temperatures. Heating has various detrimental effects on the device's performance. For example, a typical distributed Bragg reflector laser (DBR) [1] exhibits wavelength changes due to temperature fluctuations as pronounced as 0.28nm/^{0}C, however, the channel spacing for a Wavelength Division Multiplexing (WDM) system is only about 0.2~0.4nm. Thus, one or two degree temperature changes will result in crosstalk between neighboring channels. Furthermore, with increasing temperatures, the threshold current density, output power, and the spectral linewidth of optoelectronic devices will also change. In all, increasing temperatures have been the bottleneck for optoeletronics, preventing improved speed, bandwidth, and stability.

The most commonly used thermoelectric coolers are made of Bi_2Te_3. Although the absolute cooling of these commercial devices can reach 70^{0}C, however, its large device size, its leg length of at least a few mm, its low Carnot efficiency 6~8%, and the bulk fabrication technology, make it incompatible with the micro-sized optoelectronic devices. Intensive studies looking for monolithically grown micro-coolers based on III-V materials in order to realize the goal of on-chip temperature stabilization have been done [2,3,4,5,6]. However, the bulk InP and GaAs are very inefficient thermoelectronic materials. Finding an answer to the question, "how can the figure of merit for InP and GaAs be improved?", is the key to success.

Since 1993 Hicks, L.D. and Dresslhaus, M.S. showed that the thermoelectric properties could be enhanced via low dimensional structures, like superlattices and nanowires. [7,8] Since the improvement due to electron confinement in low dimensions is mainly in the plane of the multi-quantum well structure, integration with optoelectronic devices and reducing the parasitic effect of the substrate has remained a key challenge. Some researchers have been focused on cross-section superlattice microcoolers and achieved noticeable success: R. Venkatasubramanian et.al. [9] demonstrated absolute cooling of 32K at room temperature for P-type, Bi_2Te_3/Sb_2Te_3

superlattice with a ZT of 2.4; T.C. Harman et. al.[10] showed 43.7K cooling for PbSeTe/PbTe quantum dots superlattice with a ZT of 1.6; JiZhi Zhang et. al. [6] recently experimentally demonstrated AlGaAs superlattice microcooler cools 0.8C at 25^0C and 2^0C at 100^0C; UCSC/UCSB collaboration also demonstrated an N-type InP substrate based InGaAs/InP superlattice microcooler with a maximum net cooling of 2.5^0C [11]. It is likely that the enhanced cooling by the superlattice structure is a result of: (i) thermal conductivity reduction; (ii) thermionic transport by electron filtering effects. Both factors increase the figure of merit, , $ZT = \frac{S^2\sigma}{k}T$ (Eqn.1 S, Seebeck coefficient, σ, electrical conductivity, k, thermal conductivity, T, temperature). Thermal conductivity has been directly measured. Some authors have observed thermal conductivity values below bulk alloy [12,13,14,15], while Huxtable et. al. [16] did not measure this reduction for InGaAsP/InGaAs superlattice.

There are very few papers discussing how to enhance the power factor, $S^2\sigma$ perpendicular to superlattice by bandgap engineering [17,18,19,20]. Actually, the change of the Seebeck coefficient has a much more significant influence on the figure of merit, ZT, when compared with thermal conductivity, k, since S has a power factor in eqn.1. Meanwhile, the complexity of measuring the Seebeck coefficient also makes it hard. The Seebeck coefficient S is defined as equation, $S = \frac{\Delta V}{\Delta T}$ (eqn.2, ΔV, voltage difference across the junction, ΔT, the temperature difference across the junction). As long as we could measure the voltage and temperature difference accurately, the Seebeck coefficient could be calculated. The difficulty of characterizing the Seebeck coefficient of superlattice thin film lies in simultaneously measuring the voltage and temperature drop within a few microns on both sides of a thin film. We successfully measured the Seebeck coefficient by integrating a thin film heater on top of the microcooler [21]. In this paper, we chose the InGaAs/InAlAs superlattice with the higher barrier (0.54eV) to study the doping concentration and ambient temperature influence on the Seebeck coefficient. For larger barrier heterostructure superlattice devices with a short period, it is possibile to form minibands at various energy levels below and above the Fermi-energy. This can significantly affect the energy distribution of electrons moving in the materials and thus change the Seebeck coefficient.

Experiments

The heterostructure-integrated thermonic (HIT) cooler structure under test mainly consists of a superlattice layer lattice matched to an InP substrate, and a 0.5μm-thick InGaAs layer highly doped (1e19cm-3) cap layer used as the top and bottom contact layers. The superlattice contained 25 periods of 5nm thick InGaAs n-doped with varying concentrations, 2e18, 4e18, 8e18 to 3e19 cm^{-3} and 3nm thick undoped InAlAs. The whole structure was grown using metal organic chemical vapor deposition (MOCVD). Devices with various sizes were fabricated using conventional lithography, dry etching and metallization techniques. Ni/AuGe/Ni/Au was used to make ohmic contacts to both electrodes. Figure 1 shows the device's geometry under the Scanning Electron Microscope (SEM). A thin film heater was deposited on top of the microcooler and used as both heat source and temperature sensor, as illustrated in Figure 2. At last, the sample was attached to a package, wire bonded, and loaded into the cryostat.

There are total of four samples under test with different doping superlattice layers. We used two device sizes, 100x100μm2 and 70x70μm2 for measurements. First, we calibrated the heater resistance with the stage temperature. We used four-wire measurement to measure the resistance to reduce the influence of contact wires and pads. At a given heater power, the top of the cooler device was heated up by the thin film heater at a fixed temperature (T_h). The substrate was

attached to the heatsink inside the cryostat, where the temperature was controlled by the flow of liquid Helium (T_s). The temperature difference across the superlattice layer ($\Delta T=T_h-T_s$) generates a voltage difference (ΔV), which can be measured by probing the microcooler contact and ground contact. Thus, the effective Seebeck coefficient of the device could be calculated easily with eqn. 2. For the detailed calculation method to derive the Seebeck coefficient of the superlattice refers to [14]. The Seebeck coefficients were measured at cryostat temperature change from 50K to 300K.

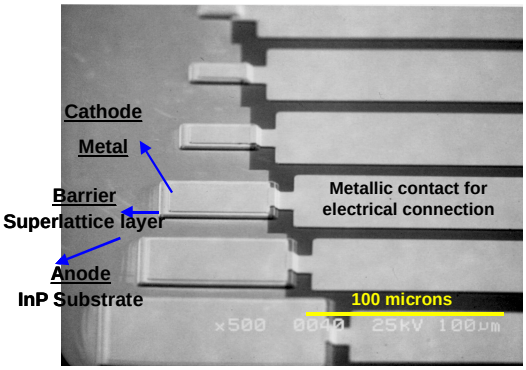

Figure 1 A Scanning Electron Microscope of device structure

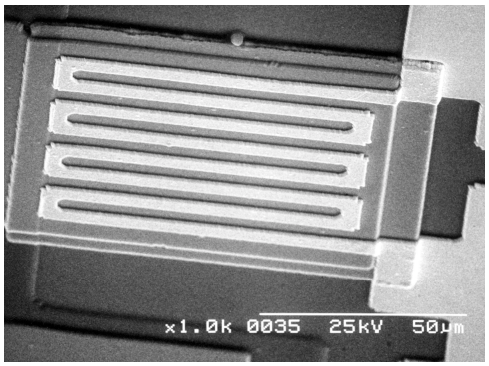

Figure 2 A Scanning Electron Microscope of the microcooler integrated with heaters

Results and Simulations

Figure 3 illustrates the measured Seebeck coefficients along with theoretical calculations for samples A, B, C, D with doping concentration ranging from 2e18, 4e18, 8e18 up to 3e19 cm^{-3}, respectively. From the graph, we can see the Seebeck coefficient increase with temperature from 10K to 300K for all samples. The graph verifies that the Seebeck coefficient is independent of device size. The Seebeck coefficient measured for both 100x100µm^2 (circles) and 70x70µm^2 (squares) size devices match except for one case. We found that the discrepancy was due to a heater fabrication error for the sample D of size100x100µm^2. The theoretical fitting was based on the model presented in [22]. For completeness we present here the basic equation with the required changes. The number of electrons that participate in a thermionic emission process can be written directly as an integral in $k_xk_yk_z$ space:

$$n_e(V)=\frac{2}{8\pi^3}\int_0^\infty dk_z\frac{\hbar^2k_z^2}{m}\int_0^\infty dk_x\int_0^\infty dk_y(-\frac{\partial f}{\partial E})T(k_x,k_y,k_z,V) \qquad \text{(eqn.3)}$$

where f is the Fermi-Dirac distribution function and V is the applied voltage across the barrier. Quantum mechanical transmission probability across the barrier, T, depends only on V, and k_z because we have assumed that the lateral momentum is conserved. The transmission probability is calculated with the use of the transfer matrix method. Since the resulting minibands' widths are in the order of or larger than the thermal energy (~20meV and 100meV for the first two minibands), a bulk-type Boltzmann transport with a correction due to quantum mechanical transmission above and below the barrier is assumed. To calculate the Seebeck coefficient, one needs to obtain the average energy transported by these electrons (n_q). The equation for the calculation of n_q is similar to Eqn. 3 except that the integrand is multiplied by the difference of the energy of emitted electrons from the Fermi level $(k_x^2+k_y^2+k_z^2-k_F^2)$. The Seebeck coefficient can be calculated from n_e and n_q according to: $S=n_q/en_eT$ where e is the charge of the electron.

This equation is a good approximation compared to more accurate definition $S = \frac{1}{T} \times \frac{J_Q}{J}$, where J_Q is the heat current transported and J is the electrical current. This is because mobility is much weaker function of electron energy than the quantum mechanical transmission probability in these superlattices in miniband transport regime. Parameters used in the calculations are listed in table I. [i] n_w is the number of superlattice periods, L_w and L_b are the widths of well and barrier, respectively, m* is the electron effective mass and α is the non-parabolicity of the conduction band.

Table I List of materials parameters

Structural parameters for the $In_{0.53}Ga_{0.47}As/In_{0.52}Al_{0.48}As$ superlattice

n_w	L_w (nm)	L_b (nm)	V_b (meV)	m*	α (ev^{-1})
250	50	30	520	0.045[23]	1.45[24]

Figure 4 illustrates the superlattice transmission coefficient as a function of electron energy. Given the finite coherence length of carriers, only two periods are taken into account. Three minibands at approximately 120, 380 and 670meV can be identified. The position of Fermi level for the four samples is also shown.

Figure 5 illustrates the theoretical prediction of the Seebeck coefficient as a function of doping concentration range along with the experimental data points (circles and squares). From the graph, we could see that the Seebeck coefficient is monotonically decreasing with doping concentrations up to 10^{19} cm^{-3}, but it starts to increase as the doping concentration is further increased. This trend was confirmed by the increased Seebeck coefficient measured for Sample D. As it can be seen in Figure 3, sample D's Seebeck coefficient is lager than bulk InGaAs doped at the same level, while Seebeck coefficients of samples A, B and C were lower than bulk values over the whole temperature range. The Seebeck coefficient of samples A and B fit the theoretical calculations with well and barrier widths of 45 and 30Å, respectively. However, sample C and D are well fitted with the well and barrier widths of 55 and 35Å, respectively. This variation could be due to the thickness variation between epitaxial growths. The thickness variation will be further investigated with the use of X-Ray diffraction that can measure accurately the superlattice period.

[i] Doping concentrations were determined to be $3x10^{18}$, $4 x10^{18}$, $7 x10^{18}$, and $2.7 x10^{19}cm^{-3}$ to fit the experimental data of samples A, B, C, and D respectively. For all samples it is assumed that only wells are doped. L_w and L_b are determined to be 55Å and 30Å for samples A and B, and 45Å and 25Å for samples C and D respectively.

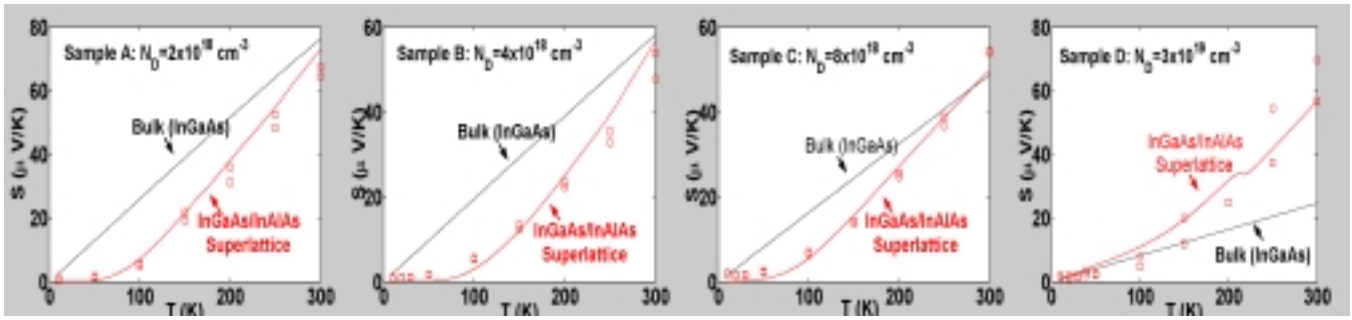

Figure 3 The measured effective Seebeck coefficient for Samples A, B, C, D (squares (device size 70x70μm^2) and circles (device size 100x100μm^2) are experimental data, the lines are theoretical modeling.

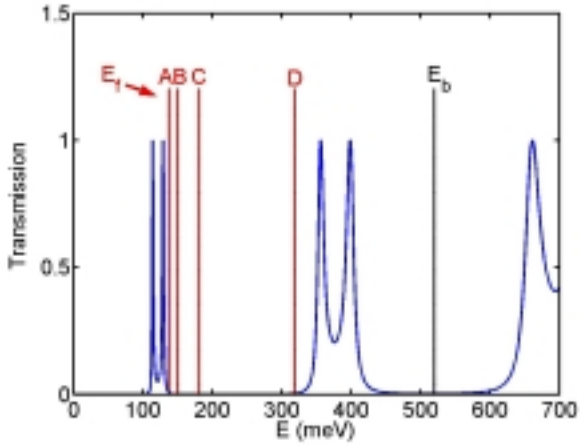

Figure 4 Superlattice transmission coefficients versus energy. Position of Fermi level for samp A, B, C and D and the barrier height are also indicated.

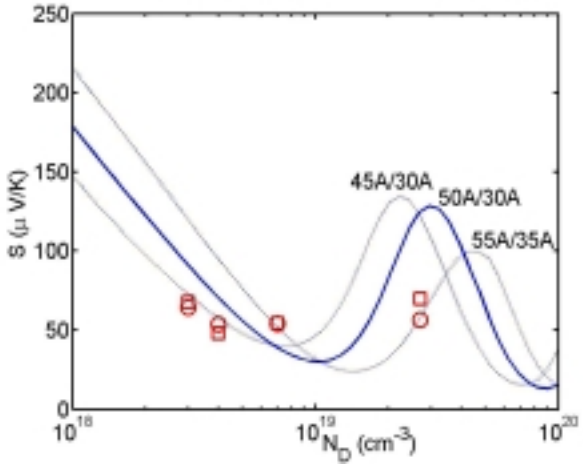

Figure 5 The theoretical Seebeck coefficient as a function of doping concentration along with the measured data for the four samples.

Discussions

Figure of Merit, ZT, of InGaAs/InAlAs superlattice with very high barriers (0.54eV) has been calculated to be up to 0.45 [25]. This value compared with the bulk ZT of InGaAs (0.04) is an order of magnitude larger. It is important to note that the benefit from superlattice could be only obtained when it is highly doped. Later calculations showed that non-planar barriers are needed to fully benefit from thermionic emission of hot carriers in tall barrier superlattices [refer to the reference: Vashaee and Shakouri, Journal of Applied Physics, 2004, Ref. 22 below]. As shown in Figure 3 for the samples A, B and C, when the doping is relatively low, the Seebeck coefficient is even lower than the bulk material. This is due to the large conduction band offset, which inhibits movement of low energy electrons. As the doping increases in a typical bulk semiconductor, Seebeck coefficient keeps decreasing. However, the experimental results in Figures 3 and 5 show that this tendency is modified due to the superlattice transport, when Fermi energy approaches the 2nd miniband.

In a superlattice it is possible to form a miniband below the Fermi-energy, as shown in Figure 6. In the case where other minibands are formed at higher energies (several times thermal

energy, kT, away from the Fermi level), electron transport above the Fermi-energy could be rejected. Thus the average energy of moving electrons should be lower than the Fermi-energy. It seems that the sign of the Seebeck coefficient could be changed compared to standard n-doped material (in which average energy of moving electrons is below Fermi level). However, we did not observe the sign change experimentally. When we carefully examined the theoretical model, we found out that only when the electron lateral momentum is not conserved during quantum mechanical transmission, the sign of the Seebeck coefficient could be changed. Lateral momentum conservation is the consequence of translational symmetry in the plane of quantum wells and it could be broken using e.g. embedded quantum dots. Calculations in Ref. 18 illustrated indeed the Seebeck coefficient sign change as p-doping increases for Ge/Si quantum dots superlattices. In the case of planar barrier, when lateral momentum is conserved, sign of the Seebeck coefficient does not change and we only see a non-monotonic variation of the Seebeck coefficient versus doping.

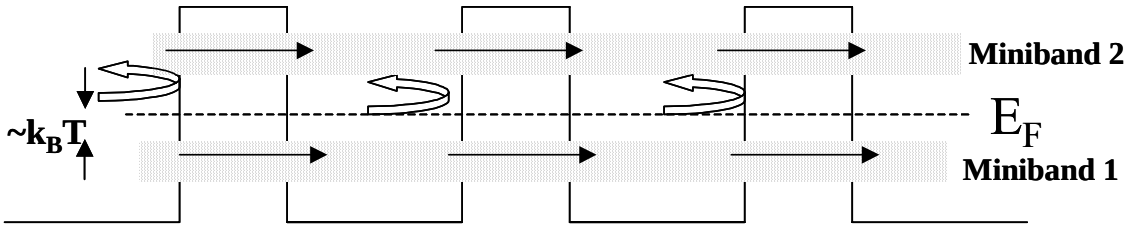

Figure 6 Schematic of miniband formation and electrons transport inside superlattice

Acknowledgement

This work was supported by the MURI TEC center program and the Packard Fellowship.

References

[1] H.B. Sequeira, "Thermoelectric properties of a Peltier cooler laser structure" Ph.D dissertation, University of Delaware, Newark, DE, 1982

[2] S. Hava, R.G. Hunsperger, and H.B. Sequeria, IEEE, J. Lightwave Tech. LT-2, 175 (1984)

[3] N.K. Dutta, T. Cellia, R. L. Brown, and D. T. C. Huo, "Monolithically integrated thermoelectric controlled laser diode", Appl. Phys. Lett 47 (3), August, 1985

[4] Daryoosh Vashaee, Christopher LaBounty, Xiaofeng Fan, Gehong Zeng, Patrick Abraham, John, E. Bowers and Alis Shakouri, "P-type InGaAsP coolers for integrated optic devices", Proceedings of the SPIE - The International Society for Optical Engineering, vol.4284, (Functional Integration of Opto-Electro-Mechanical Devices and Systems) p.139-44, San Jose, CA, 20-26 January 2001

[5] Chris LaBounty, Daryoosh Vashaee, Xiaofeng Fan, Gehong Zeng, Patrick Abraham, Ali Shakouri, John E. Bowers, **"**P-type InGaAs/InGaAsP Superlattice Coolers**"**, 19th International Conference on Thermoelectrics, Cardiff, Wales, August 2000

[6] Jizhi Zhang, Neal G. Anderson, and Kei May Lau, "AlGaAs superlattice microcoolers", Applied Physics Letters, Vol.83, No.2, P374, July, 2003

[7] Hicks, L.D. and Dresselhaus, M.S., "Effect of quantum-well structures on the thermoelectric figure of merit", Phys. Rev. B, Vol.47, No.19, P12727, 1993

[8] Hicks, L.D. and Dresselhaus, M. S., "Thermoelectric figure of merit of a one-dimensional conductor", Phys. Rev. B, Vol. 47, No. 24, P16631, 1993

[9] R. Venkatasubramanian, E. Silvola, and T. Colpitts, "Thin-film thermoelectric devices with high room-temperature figures of merit", Nature, Vol. 413, P597, 2001
[10] T. C. Harman, P. J. Taylor, M. P. Walsh and B.E. LaForge, "Quantum Dot Superlattice Thermoelectric Materials and Devices", Science, Vol. 297, P2229, 2002
[11] Yan Zhang, James Christofferson, Daryoosh Vashaee, Phuong Nguyen, Ali Shakouri, Gehong Zeng, Chris Labounty, Yae Okuno, Yi-Jen Chiu, and John E. Bowers, "Thin film coolers for localized temperature control in optoelectronic integrated circuits", Proceeding of 53rd ECTC, P312, New Orleans, LA, May, 2003
[12] W.S. Capinski and H.J. Maris, "Thermal conductivity of GaAs/AlAs superlattices", Physica B Vol. 219&220, P699, 1996
[13] B.Yang, W.L. Liu, J.L. Liu, K.L. Wang and G. Chen, "Measurements of anisotropic thermoelectric properties insuperlattices", Applied Physics Letters, Vol. 81, No. 19, 2002
[14] Chen, G., "Thermal Conductivity and Ballistic Phonon Transport in Cross-Plane Direction of Superlattices," Phys. Rev. B, 57 P14958, 1998
[15] G. Chen and Ali Shakouri, "Heat Transfer in Nanostructures for Solid-State Energy Conversion", Journal of Heat Transfer, Vol. 124, P242, 2002
[16] Scott Huxtable, Ali Shakouri, Patrick Abraham, Yi-Jen Chiu, Xiaofeng Fan, John E. Bowers and Arun Majumdar, "Thermal conductivity of Indicum Phosphide based superlattices", Proceeding of 18th International Confereence on Thermoelectrics, P594, 1999
[17] T. Koga, X. Sun, S.B. Cronin and M.S. Dresselhaus, "Carrier pocket engineering to design superior thermoelectric materials using GaAs/AlAs superlattices", Appl. Phys. Lett., Vol. 73, No.20, P2950, 1998
[18] Alexander A. Balandin and Olga L. Lazarenkova, "Mechanism of thermoelectric figure-of-merit enhancement in regimented quantum dot superlattices", Appl. Phys. Lett., Vol. 82, No.3, P415, 2003
[19] D.M. Rowe, and G. Min, "Multiple potential barriers, as a possible mechanism to increase the Seebeck coefficient and electrical power factor", Thirteenth International Conference on Thermoelectrics, Kansas City, pp339, 1994
[20] L.W. Whitlow, and T. Hirano, "Superlattice applications to thermoelectricity", Journal of Applied Physics, Vol, 78, P5460, 1995
[21] Zhang, Y.; Zeng, G.; Singh, R.; Christofferson, J.; Croke, E.; Bowers, J.E.; Shakouri, A. "Measurement of Seebeck coefficient perpendicular to SiGe superlattice layers," 21st International Conference on Thermoelectrics, Long Beach CA, 26-29 August 2002.
[22] D.Vashaee, and A. Shakouri, "Electronic and Thermoelectric Transport in Semiconductor and Metallic Superlattices", Submitted for publication to Journal of Applied Physics.
[23] K. Tanaka, N. Kotera, H. Nakamura, "Nonparabolic tendency of electron effective mass estimated by confined states in $In_{0.53}Ga_{0.47}As/In_{0.52}Al_{0.48}As$ multi-quantum-well structures". Superlattices and Microstructures, Vol. 26, No. 1, 1999.
[24] Pau Garcias-Salvà, Lluís Prat Viñas, "Inclusion of the Conduction Band non-Parabolicity in the Monte Carlo Simulation of Abrupt HBTs".
[25] Ali Shakouri, Chris LaBounty, Patrick Abraham, Joachim Piprek, and John E. Bowers, "InP-based thermoinc coolers", 11th Internation Conference on Indium Phosphide and Related Materials, May, 1999, Davos, Switzerland